HHS Public Access

Author manuscript

*Skeletal Radiol*. Author manuscript; available in PMC 2023 March 01.

Published in final edited form as:

*Skeletal Radiol*. 2022 March ; 51(3): 549–556. doi:10.1007/s00256-021-03848-y.

# Clinical Utility of Accelerated MAVRIC-SL with Robust-PCA Compared to Conventional MAVRIC-SL in Evaluation of Total Hip Arthroplasties.

**Zoe Doyle**[1,*], **Daehyun Yoon**[1,*], **Philip K. Lee**[1,2], **Jarrett Rosenberg**[1], **Brian A. Hargreaves**[1,2,3], **Christopher F. Beaulieu**[1,4], **Kathryn J. Stevens**[1,4]

[1]Department of Radiology, Stanford University, Stanford, CA 94305.

[2]Department of Electrical Engineering, Stanford University, Stanford, CA 94305

[3]Department of Bioengineering, Stanford University, Stanford, CA 94305

[4]Department of Orthopaedic Surgery, Stanford University, Redwood City, CA 94063

## Abstract

**Objective.—**To compare the diagnostic performance of a conventional metal artifact suppression sequence MAVRIC-SL (multi-acquisition variable-resonance image combination selective) and a novel 2.6-fold faster sequence employing robust principal component analysis (RPCA), in the MR evaluation of hip implants at 3T.

**Materials and Methods.—**36 total hip implants in 25 patients were scanned at 3T using a conventional MAVRIC-SL proton density-weighted sequence and an RPCA MAVRIC-SL proton density-weighted sequence. Comparison was made of image quality, geometric distortion, visualization around acetabular and femoral components, and conspicuity of abnormal imaging findings using the Wilcoxon signed-rank test and a non-inferiority test. Abnormal findings were correlated with subsequent clinical management and intraoperative findings if the patient underwent subsequent surgery.

**Results.—**Mean scores for conventional MAVRIC-SL were better than RPCA MAVRIC-SL for all qualitative parameters ($p < 0.05$), although the probability of RPCA MAVRIC-SL being clinically useful was non-inferior to conventional MAVRIC-SL (within our accepted 10% difference, $p < 0.05$), except for visualization around the acetabular component. Abnormal imaging findings were seen in 25 hips, and either equally visible or visible but less conspicuous on RPCA MAVRIC-SL in 21 out of 25 cases. In 4 cases a small joint effusion was queried on MAVRIC-SL but not RPCA MAVRIC-SL, but the presence or absence of a small effusion did not affect subsequent clinical management and patient outcome.

**Conclusion.—**While overall image quality is reduced, RPCA MAVRIC-SL allows for significantly reduced scan time and maintains almost equal diagnostic performance.

**Correspondence:** Name: Kathryn J. Stevens, Address: Department of Radiology, Center for Academic Medicine Radiology, 453 Quarry Road, Palo Alto, CA 94304., kate.stevens@stanford.edu, Fax: (650) 725-7296, Telephone: (650) 725-8638.

*First authorship is shared by Zoe Doyle and Daehyun Yoon. Both individuals contributed substantially and equally to study design, data acquisition, analysis, and interpretation, and manuscript writing.

**Keywords**

Magnetic Resonance Imaging; Hip; Arthroplasty; Replacement; Principal Component Analysis

## Introduction

Imaging is key to diagnosing complications of total hip arthroplasty, which include aseptic loosening, periprosthetic fracture, infection, hardware failure, and adverse local tissue reaction [1]. Radiographs are usually the first choice in assessment of painful hip replacements, but when they fail to identify any abnormal findings, MRI is often the best choice for further evaluation, particularly when adverse local tissue reaction is suspected or if the pain generator is suspected to be in the extra-articular soft tissues [2–4].

Unfortunately, MRI evaluation can be challenging due to artifacts induced by metallic implants, including significant signal loss, pile-up artifact and geometric distortion, which obscure visualization of adjacent anatomic structures [5]. Despite greater susceptibility artifact at 3T compared to 1.5T, market demand for higher strength MRI scanners continues to grow due to its speed and often superior imaging quality, and as imaging centers update their equipment, 3T scanners are increasingly used, which will create the need for improved metal suppression techniques at higher field strengths [6].

Metal artifact reduction sequence (MARS) MRI combined a few strategies to correct for in-plane directional distortions [7]. Following MARS, a number of 3D multi-spectral imaging (MSI) approaches were developed and demonstrated substantial suppression of metal-induced artifacts for both in-plane and through-plane directions [8–15]. These 3D MSI sequences were initially validated for 1.5T MRI, but later showed the feasibility of comparable artifact correction for 3T MRI [16, 17]. However, additional slice-encoding and multi-spectral acquisition adopted in these techniques result in long scan times despite the use of many standard acceleration techniques [14, 18], which can still be difficult for symptomatic elderly patients with postoperative complications to tolerate.

Recently, a novel compressed-sensing algorithm for MAVRIC-SL exploiting the redundancy of the spectral bins and sparsity of off-resonance signals with robust principal component analysis (RPCA MAVRIC-SL) presented promising results in additional scan time reduction in a small set of patients [19]. The technique exploits the sparsity of off-resonance and the structure of the dominant on-resonance component: at fixed z-locations in space, spectral bin profiles for the dominant on-resonance component are related only by scaling. The joint reconstruction approach for spectral bins of RPCA MAVRIC-SL facilitated a greater scan time reduction than conventional compressed-sensing approaches that reconstruct each spectral bin independently [20, 21]. Our study aims to determine whether accelerated RPCA MAVRIC-SL offers similar diagnostic performance compared to conventional MAVRIC-SL at 3T in hip arthroplasty patients.

## Materials and Methods

### Patient Selection

Patients referred for evaluation of symptomatic total hip implants were recruited between October 2017 and March 2017. Patients with standard MRI contraindications such as claustrophobia, intracranial aneurysm clips or MRI-incompatible devices were excluded. Twenty-five patients (9 males, 16 females) aged 52–82 years (mean 68 years) were included in the study. Fourteen patients had unilateral hip implants and 11 had bilateral implants, at least one of which was symptomatic, giving a total of 36 hip replacements. Prior to imaging, all patients signed an informed consent form approved by the institutional review board to have RPCA MAVRIC-SL added to their routine imaging metal artifact reduction protocol of the hip, which had included coronal STIR MAVRIC SL, coronal T1, axial STIR, and axial T1 in all patients.

### Image Acquisition

Coronal proton density-weighted MAVRIC-SL and RPCA MAVRIC-SL images were acquired on a GE Discovery MR750 3T scanner (GE Healthcare, Waukesha, WI, USA) using a 32-channel torso array coil whose top and bottom units were placed over and under the patient, respectively. A non-fat saturated proton density-weighted sequence was selected to facilitate comparison of anatomic detail as well as depiction of joint pathology. Scan parameters were as follows: TR/TE 4s/6.6ms, FOV 36x36 cm, image matrix size 384x256, slice thickness 4mm, number of slices 24, readout bandwidth ±125KHz, number of spectral bins 24, spectral coverage 24KHz, echo train length 20. Conventional MAVRIC-SL was acquired using 2x2 autocalibrating parallel imaging, and RPCA MAVRIC-SL was acquired using complementary Poisson-disc sampling configured to achieve 2.6-fold extra acceleration compared to the conventional MAVRIC-SL [19]. Mean acquisition time was 6 minutes for conventional MAVRIC-SL and 2.3 minutes for RPCA MAVRIC-SL.

### Image Analysis

Anonymized conventional MAVRIC-SL and RPCA MAVRIC-SL images were independently reviewed by two fellowship-trained musculoskeletal radiologists (21 and 25 years of experience respectively) without knowledge of the patient's subsequent clinical management or operative findings. Images were reviewed in pairs for each patient to increase sensitivity in detecting small differences. Annotations were removed and the order in which MAVRIC-SL and RPCA MAVRIC-SL sequences were presented were randomized within each pair. Images were scored on a 5-point scale for image quality and geometric distortion, using the scoring system described by Nardo et al with small modifications (Table 1) [16]. Image quality was determined by assessing all slices of the sequence, with particular attention to overall image sharpness and contrast.

Geometric distortion was defined as the degree of signal loss and pile-up artifact related to the implant obscuring the normal anatomic contours. This was further subdivided into geometric distortion relating to the femoral and acetabular components, which were also assigned individual scores. The total extent of artifact on matching slices was quantitatively

determined by drawing an ROI around the total area of signal loss and pile-up artifact surrounding the hip implant on the slice with maximal artifact.

Images were also evaluated for the presence or absence of abnormal findings including joint effusion, capsular thickening, periprosthetic signal abnormality, periarticular fluid collections or soft tissue masses (pseudotumors), tendon pathology and fracture. The degree of confidence with which the presence or absence of abnormal findings were identified was evaluated using a 4-point scale, defined in Table 1. The patient's electronic medical records were accessed after the image analysis to determine the subsequent clinical management, and any intra-operative findings if available. Imaging abnormalities seen on the coronal proton density-weighted MAVRIC-SL and RPCA MAVRIC-SL were compared with findings from the original MRI studies, which had been acquired at the same time in all patients and included a number of additional metal artifact reduction sequences including coronal STIR MAVRIC SL, coronal T1, axial STIR, and axial T1.

## Statistical tests

The two-sided Wilcoxon signed-rank test was used to compare the scores between RPCA MAVRIC-SL and MAVRIC-SL for overall image quality, geometric distortion, and quantitative extent of artifact. The presence of suspected clinical pathology, i.e. abnormal imaging findings, was not compared using a statistical test because both low and high scores can indicate strong confidence (Table 1). Instead, the frequencies of concordance and discordance between the scores of the two compared image sets were measured. Interobserver agreement was determined using Gwet's agreement coefficient [22] and its 95% confidence interval.

We assumed that the scores of RPCA MAVRIC-SL images could either be equal or lower to those of conventional MAVRIC-SL images due to potential SNR loss from adopting a higher data under-sampling rate or blurring artifacts from RPCA reconstruction [19], but hypothesized that the difference would not be sufficient to affect the diagnostic accuracy of the scan. Therefore, we conducted a non-inferiority test to evaluate the clinical usefulness of RPCA MAVRIC-SL compared to conventional MAVRIC-SL. For each score (overall image quality, geometric distortion, visualization around the acetabular component, and visualization around the femoral component), the probability of a "clinically useful" rating was estimated by logistic regression on the imaging method (conventional vs RPCA) adjusted for clustering effects within patients having bilateral hip replacements. The original 5-point scale ratings were dichotomized to be regarded as either "clinically useful" (a score higher than or equal to 3) or "not clinically useful" (a score less than 3). The model's estimated difference between the two methods' probabilities was compared to a non-inferiority limit of −0.10 (−0.10 indicates the probability of RPCA MAVRIC-SL being clinically useful is 10% less than that of conventional MAVRIC-SL).

## Results

### Image quality

Mean scores for RPCA MAVRIC-SL were lower compared to conventional MAVRIC-SL, particularly with regard to image quality, with a p-value of <0.05 in all cases, although the absolute differences between mean scores were <1 for all parameters (Figure 1, Table 2). Non-inferiority testing demonstrated that the difference in probabilities of achieving a clinically useful image quality between the two sequences is estimated to range within our accepted threshold of 10%, except for visualization around the acetabular component (Figure 2). It should be noted that the estimated difference in visualization around the acetabulum was 6.9% and it was only the lower bound of its confidence interval that exceeded the accepted threshold. For both readers combined, visualization around the acetabular component was suboptimal and graded as 2 in 17% of MAVRIC SL studies and 28% of RPCA MAVRIC SL studies. Visualization around the femoral component in comparison was considered as suboptimal in 3% of MAVRIC SL studies and 8% of RPCA MAVRIC SL studies. Although overall image quality was graded as higher in the conventional MAVRIC SL images, the differences were often minimal when compared side by side (Figures 3 and 4). Figure 5 shows examples where image quality was graded identically for both sequences.

### Interobserver agreement

Interobserver agreement ranged from 0.78–0.98 (substantial to almost perfect agreement) and is presented in Table 3 with the associated confidence intervals. The lowest agreement coefficient was for visualization around the femoral component on RPCA MAVRIC-SL (0.78), and the highest was for geometric distortion on conventional MAVRIC-SL (0.98). The difference of the artifact extent measured using ROI was not found to be statistically significant between the two methods ($p = 0.07$), averaging 54.2 $cm^2$ for RPCA MAVRIC-SL and 52.8 $cm^2$ for MAVRIC-SL.

Identical scores were given to the presence or absence of abnormal imaging findings in conventional MAVRIC-SL and RPCA MAVRIC-SL by at least one observer in 33 of the 36 cases; scoring was concordant for both observers in 27. Abnormal imaging findings were seen in 25 hips (scores of 3 or 4), comprising joint effusions in 21, iliopsoas or peritrochanteric pseudotumors in 14, capsular thickening in 1, and gluteal tendon pathology in 1. No fractures or abnormal periprosthetic bone marrow signal were identified in our cohort. In 9 cases where scoring between conventional and RPCA images was discordant, there were 5 hips where at least one observer identified pathology more confidently on conventional MAVRIC-SL (score of 4) compared to RPCA images (score of 3). In 2 of these the abnormal finding was a small joint effusion and both patients were subsequently followed clinically. In the other 3 cases the abnormal imaging findings were small joint effusions and trochanteric fluid collections (Figure 6); one of these patients was subsequently revised for adverse local tissue reaction, one underwent arthroplasty resection for infection, and in the other the trochanteric fluid collection had decreased on a follow up ultrasound so the patient declined surgery and elected to be followed up clinically.

In the four cases with discordant scores of 2 on RPCA MAVRIC SL vs 3 on conventional MAVRIC-SL, the probable abnormalities seen on conventional MAVRIC-SL were all small joint effusions.

### Patient follow-up

Of the 36 hips in the study, 8 hips were subsequently revised for adverse local tissue reaction and in all but one of these cases a trochanteric or iliopsoas pseudotumor was diagnosed by both readers on both sequences. In the one case that a pseudotumor was not identified, a trace trochanteric fluid collection was identified on the axial short tau inversion recovery (IR) and coronal MAVRIC SL-IR images of the original diagnostic protocol.

## Discussion

RPCA MAVRIC-SL is a novel MR technique that uses a pseudorandom sampling pattern and regularized reconstruction to accelerate conventional MAVRIC-SL, allowing for 2.6x faster scanning, which can be advantageous in patients unable to tolerate long examination times, and also has the potential to increase patient throughput, particularly if the technique can be applied to multi-planar multisequence imaging protocols. This study compared the imaging quality, metal artifact suppression, and clinical utility of RPCA MAVRIC-SL and conventional MAVRIC-SL in patients with hip implants.

Although the scores for overall image quality and visualization around the femoral component were lower for RPCA MAVRIC-SL compared to conventional MAVRIC SL, the clinical usefulness of the two techniques based on non-inferiority testing was not significantly different. Subjective geometric distortion from metallic artifact was greater with the RPCA technique, although differences fell within a very small tolerance range and were almost negligible. In contrast to the femoral component, visualization of anatomy around the acetabular component was poorer on RPCA images. Although the difference in probability of a clinically useful scan was still within our accepted range for visualization around the acetabular component, the lower bounds of the confidence intervals fell outside our threshold. This was likely because geometric distortion around the acetabular component was much greater in some patients, possibly due to implant composition and design. Unfortunately, specific details of the type of implant and corresponding radiographs were not available in these patients, as many of the scan requests came from an outside referrer. Further investigation is needed if the increased artifact extent could be mitigated by customizing parameters of the RPCA reconstruction process.

Abnormal imaging findings, which included capsular thickening, pseudotumors or fluid collections, and joint effusions, were mostly well seen using both imaging techniques, with some more confidently identified on the conventional MAVRIC-SL images, although still visible with the RPCA technique. The presence of imaging abnormalities was identified with equal frequency, with the exception of 4 cases in which a possible joint effusion was queried on conventional MAVRIC-SL, but not on RPCA MAVRIC-SL. However, diagnosis of a joint effusion can be subjective, as a small amount of joint fluid may be physiologic. Review of these patients' medical records indicated that the presence or absence of a small joint effusion would not have affected the patient's subsequent clinical management.

Although we did not anticipate that using only coronal PD-weighted images would be highly sensitive in detecting pathology, on subsequent review of the original diagnostic MRI studies, there was only one case in which an additional imaging abnormality was identified. This was a thin T2 hyperintense peritrochanteric fluid collection which was only seen on axial STIR and MAVRIC SL-IR images, and even in retrospect could not be identified on the coronal proton density-weighted images in our current study.

Prior studies have evaluated the clinical benefit of MAVRIC techniques at both 1.5 and 3T [13, 16, 23, 24]. Nardo et al compared MAVRIC-SL at 1.5 and 3T and found that although image quality was better at 1.5 T, visualization of anatomic structures and clinical abnormalities was not significantly different between the two field strengths [16]. However, scan times for conventional MAVRIC-SL are long, particularly when routine protocols consist of multiple sequences acquired in orthogonal planes, and extended scan times may be difficult for symptomatic patients to tolerate, resulting in motion artifact. Results of the current study show a reduction in image quality and increased geometric distortion with RPCA MAVRIC-SL and are consistent with those in the study by Levine et al [19], which used similar parameters comparing the same sequences in a smaller cohort of 8 patients. This work expands upon the prior study by examining the clinical utility of RPCA MAVRIC-SL compared to conventional MAVRIC-SL, with a focus on identifying arthroplasty complications and correlating this with subsequent clinical outcomes and surgical findings where applicable.

Limitations of our study included the small sample size, and future studies should include larger patient cohort with greater number and range of associated pathologies. Radiologists were aware that the task was to compare a conventional and accelerated sequence, which introduces inherent bias, particularly as the RPCA MAVRIC-SL images were a little more blurry than conventional MAVRIC-SL. However, all annotations and identifying data were removed from the images, and within each pair, sequences were reviewed in random order to minimize bias. Review of paired images was by design due to the subjective nature of visual assessment, as it was the authors' belief that small differences in image quality and distortion were only perceptible with side-by-side comparison and would otherwise be lost in a totally randomized process. Another limitation is that 11 of the patients had bilateral hip implants; however, each side was reviewed independently, and our statistical test adjusted for potential effects of clustering in these patients. In addition, many of the patients in this study were sent by an outside referrer, and the patient's original surgery notes and radiographs were unavailable. We were therefore unable to determine the different types and composition of the total hip arthroplasties, which may have affected the degree of susceptibility artifact generated around some of the components, causing some to be rated as not clinically useful.

In conclusion, the likelihood of the RPCA MAVRIC-SL sequence being clinical useful when compared to the conventional MAVRIC-SL is estimated to range within our accepted threshold for almost all parameters. The proposed 2.6-fold accelerated RPCA MAVRIC-SL sequence maintained nearly equivalent diagnostic accuracy in detection of implant-related complications which suggests that it would confer comparable clinical benefit when included or substituted in a standard imaging protocol. The faster scan time of RPCA

MAVRIC-SL at 3T has the potential to decrease patient discomfort, thereby minimizing motion artifact during MRI exams while simultaneously improving patient throughput.

## Acknowledgements

We thank Dr. Evan Levine for assistance in the design of the RPCA MAVRIC-SL sequence. This work was supported by the National Institutes of Health (R01 EB017739) and GE Medical Systems.

### Funding information

National Institute of Biomedical Imaging and Bioengineering R01 EB017739, GE Healthcare.

## References

1. Hargunani R, Madani H, Khoo M, et al. Imaging of the Painful Hip Arthroplasty. Can Assoc Radiol J 2016;67(4):345–355. [PubMed: 27221697]
2. Fritz J, Lurie B, Miller TT, Potter HG. MR imaging of hip arthroplasty implants. Radiographics 2014;34(4):E106–132. [PubMed: 25019450]
3. Potter HG, Nestor BJ, Sofka CM, Ho ST, Peters LA, Salvati EA. Magnetic resonance imaging after total hip arthroplasty: evaluation of periprosthetic soft tissue. J Bone Joint Surg Am 2004;86(9):947–54.
4. Walde TA, Weiland DE, Leung SB, et al. Comparison of CT, MRI, and radiographs in assessing pelvic osteolysis: a cadaveric study. Clin Orthop Relat Res 2005;(437):138–44.
5. Talbot BS, Weinberg EP. MR Imaging with Metal-suppression Sequences for Evaluation of Total Joint Arthroplasty. Radiographics 2016;36(1):209–225. [PubMed: 26587889]
6. Chang KJ, Kamel IR. Body MR imaging at 3T: basic considerations about artifacts and safety. In: Kamel IR, Merkle EM, eds. Body MR Imaging at 3 Tesla Cambridge: Cambridge University Press; 2011;1–11. doi:10.1017/CBO9780511978968.
7. Olsen RV, Munk PL, Lee MJ, et al. Metal artifact reduction sequence: early clinical applications. Radiographics 2000;20(3):699–712. [PubMed: 10835123]
8. Koch KM, Brau AC, Chen W, et al. Imaging near metal with a MAVRIC-SEMAC hybrid. Magn Reson Med 2011;65(1):71–82. [PubMed: 20981709]
9. Koch KM, Lorbiecki JE, Hinks RS, King KF. A multispectral three-dimensional acquisition technique for imaging near metal implants. Magn Reson Med 2009;61(2):381–390. [PubMed: 19165901]
10. Lu W, Pauly KB, Gold GE, Pauly JM, Hargreaves BA. SEMAC: Slice Encoding for Metal Artifact Correction in MRI. Magn Reson Med 2009;62(1):66–76. [PubMed: 19267347]
11. Hargreaves BA, Worters PW, Pauly KB, Pauly JM, Koch KM, Gold GE. Metal-induced artifacts in MRI. AJR Am J Roentgenol 2011;197(3):547–555. [PubMed: 21862795]
12. Harris CA, White LM. Metal artifact reduction in musculoskeletal magnetic resonance imaging. Orthop Clin North Am 2006;37(3):349–359, vi. [PubMed: 16846766]
13. Kretzschmar M, Nardo L, Han MM, et al. Metal artefact suppression at 3 T MRI: comparison of MAVRIC-SL with conventional fast spin echo sequences in patients with Hip joint arthroplasty. Eur Radiol 2015;25(8):2403–2411. [PubMed: 25680728]
14. Otazo R, Nittka M, Bruno M, et al. Sparse-SEMAC: rapid and improved SEMAC metal implant imaging using SPARSE-SENSE acceleration. Magn Reson Med 2017;78(1):79–87. [PubMed: 27454003]
15. Wiens CN, Artz NS, Jang H, McMillan AB, Reeder SB. Externally calibrated parallel imaging for 3D multispectral imaging near metallic implants using broadband ultrashort echo time imaging. Magn Reson Med 2017;77(6):2303–2309. [PubMed: 27403613]
16. Nardo L, Han M, Kretzschmar M, et al. Metal artifact suppression at the hip: diagnostic performance at 3.0 T versus 1.5 Tesla. Skeletal Radiol 2015;44(11):1609–1616. [PubMed: 26201676]

17. Liebl H, Heilmeier U, Lee S, et al. In vitro assessment of knee MRI in the presence of metal implants comparing MAVRIC-SL and conventional fast spin echo sequences at 1.5 and 3 T field strength. J Magn Reson Imaging 2015;41(5):1291–9. [PubMed: 24912802]

18. Hargreaves BA, Chen W, Lu W, et al. Accelerated slice encoding for metal artifact correction. J Magn Reson Imaging 2010;31(4):987–996. [PubMed: 20373445]

19. Levine E, Stevens K, Beaulieu C, Hargreaves B. Accelerated three-dimensional multispectral MRI with robust principal component analysis for separation of on- and off-resonance signals. Magn Reson Med 2018;79(3):1495–1505. [PubMed: 28686800]

20. Fritz J, Ahlawat S, Demehri S, et al. Compressed Sensing SEMAC: 8-fold Accelerated High Resolution Metal Artifact Reduction MRI of Cobalt-Chromium Knee Arthroplasty Implants. Invest Radiol 2016;51(10):666–676. [PubMed: 27518214]

21. Worters PW, Sung K, Stevens KJ, Koch KM, Hargreaves BA. Compressed-sensing multispectral imaging of the postoperative spine. J Magn Reson Imaging 2013;37(1):243–248. [PubMed: 22791572]

22. Gwet KL. Computing inter-rater reliability and its variance in the presence of high agreement. Br J Math Stat Psychol 2008;61(Pt 1):29–48. [PubMed: 18482474]

23. Hayter CL, Koff MF, Shah P, Koch KM, Miller TT, Potter HG. MRI after arthroplasty: comparison of MAVRIC and conventional fast spin-echo techniques. AJR Am J Roentgenol 2011;197(3):W405–11. [PubMed: 21862766]

24. Choi SJ, Koch KM, Hargreaves BA, Stevens KJ, Gold GE. Metal artifact reduction with MAVRIC SL at 3-T MRI in patients with hip arthroplasty. AJR Am J Roentgenol 2015;204(1):140–7 [PubMed: 25539249]

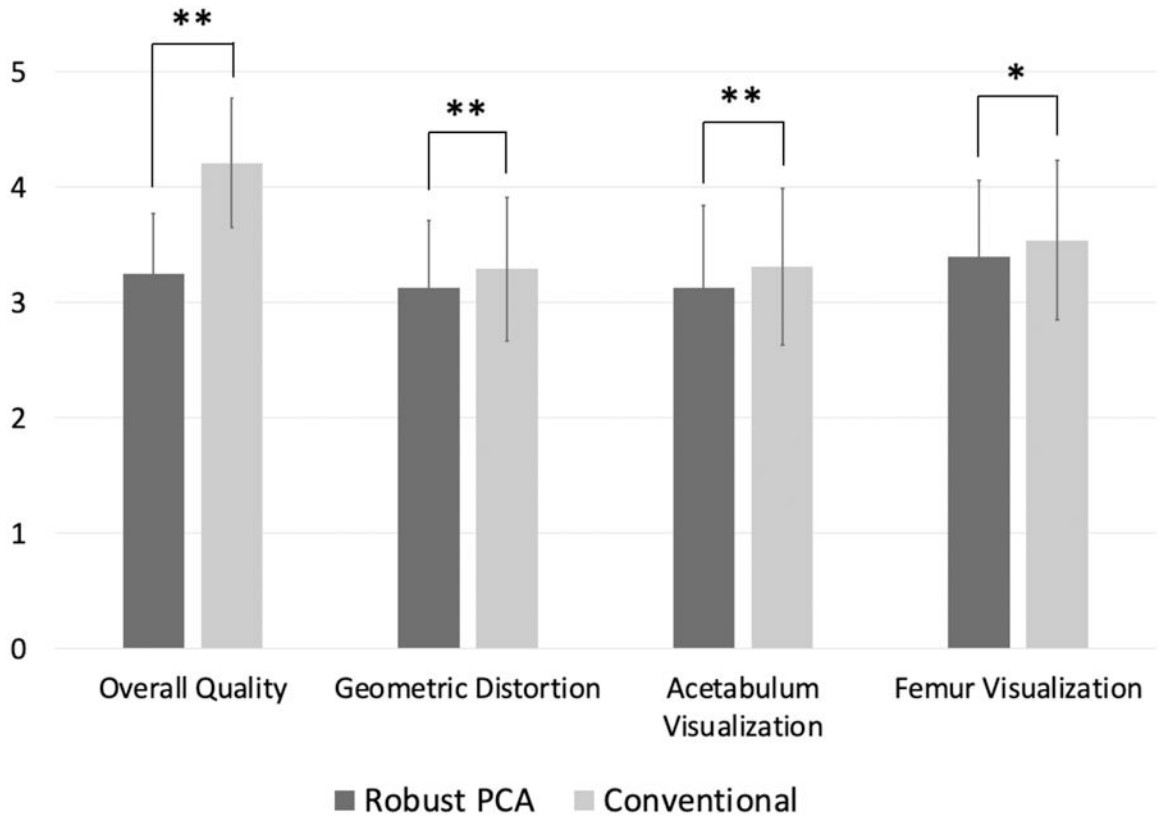


**Figure 1.**

Comparison of mean scores for qualitative parameters. ** is for the p-value less than 0.01 and * is for the p-value less than 0.05 from the two-sided Wilcoxon signed-rank test. Mean scores for conventional MAVRIC-SL were higher compared to RPCA MAVRIC-SL, although differences between the means was <1 for all parameters.

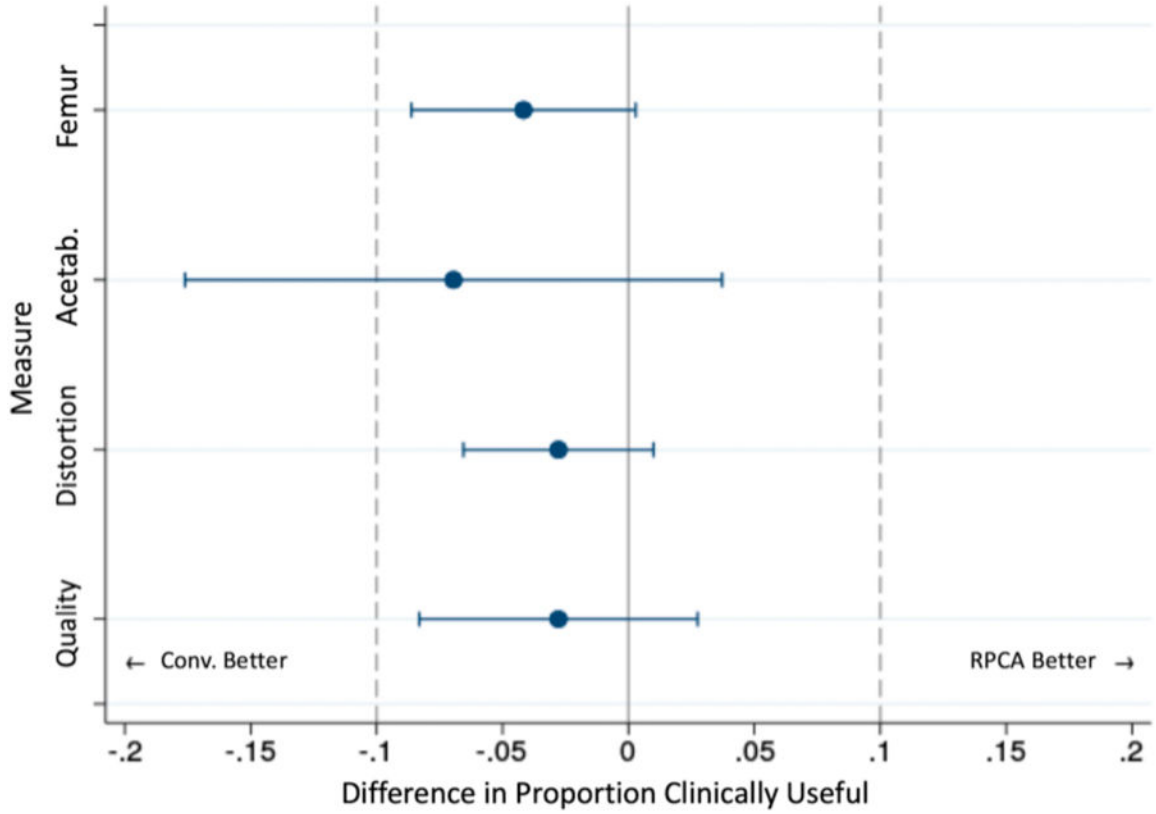


**Figure 2.**

Difference of the probabilities of clinical usefulness. Logistic regression was performed to estimate the 95% confidence interval of the probability difference for each measure. Except for acetabular visualization, the lower bounds of the confidence intervals were larger than our threshold of −0.1, suggesting non-inferiority of RPCA MAVRIC-SL to the conventional method with $p < 0.05$.

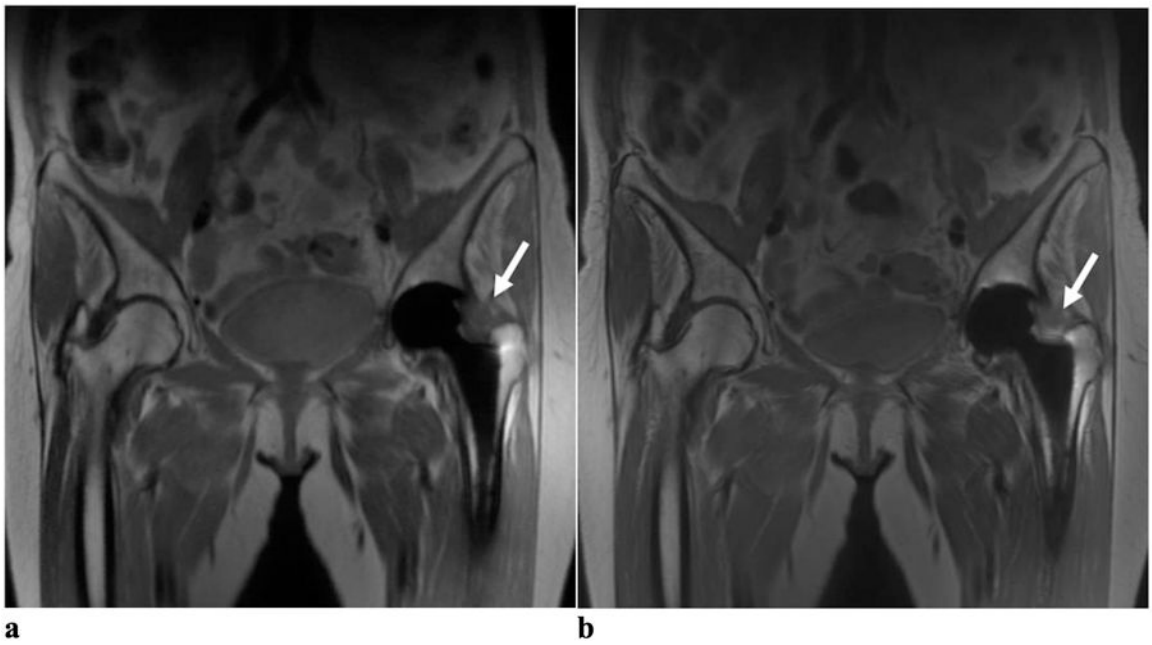


**Figure 3.**

(a) Coronal RPCA MAVRIC-SL and (b) Coronal MAVRIC-SL PD images in a 67-year-old female with left hip pain. Both readers graded the RPCA MAVRIC-SL sequence as 4 for overall image quality and the conventional MAVRIC-SL as 5. Both readers graded the geometric distortion and visualization of anatomy around the femoral and acetabular components as 4 for both sequences. Both readers thought that a joint effusion with capsular thickening was definitely present (arrows) in both images with a small trochanteric fluid collection (not shown).

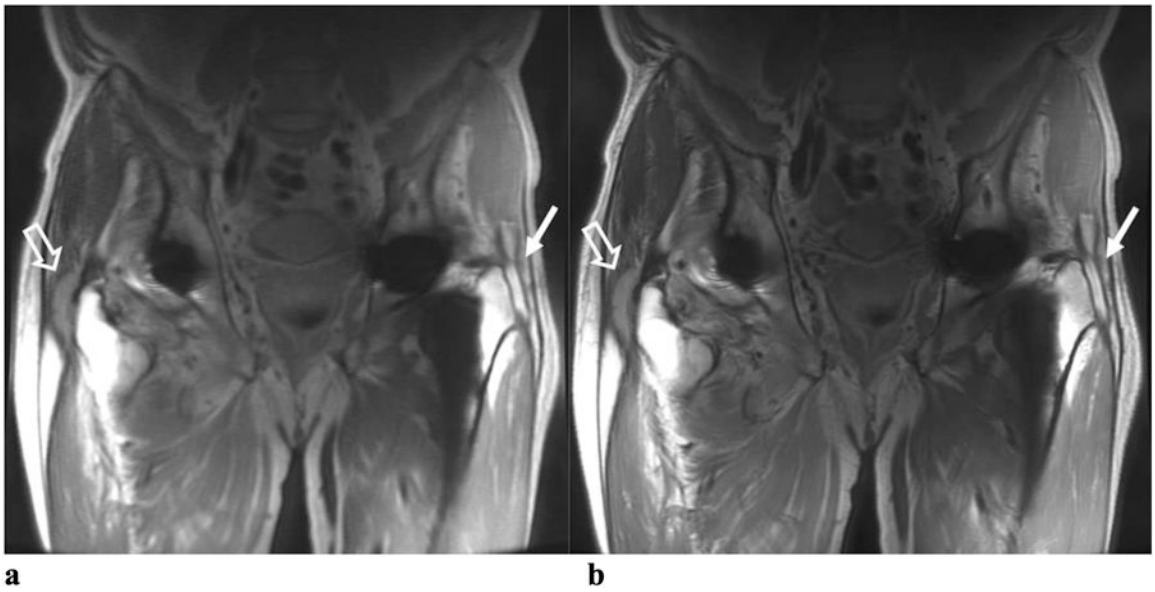


**Figure 4.**

(a) Coronal RPCA MAVRIC-SL and (b) Coronal MAVRIC-SL PD images in a 72-year-old male with bilateral hip pain. Both readers graded the overall image quality for the RPCA technique as 3 and the conventional MAVRIC-SL as 4. Reader One thought that a trochanteric fluid collection was probably present on the left (solid arrows) in both sequences, whereas Reader Two thought that a definite trochanteric fluid collection was present in both. Both readers said that a definite complex, thick-walled trochanteric fluid collection was present on the patient's right (open arrows) on both sequences.

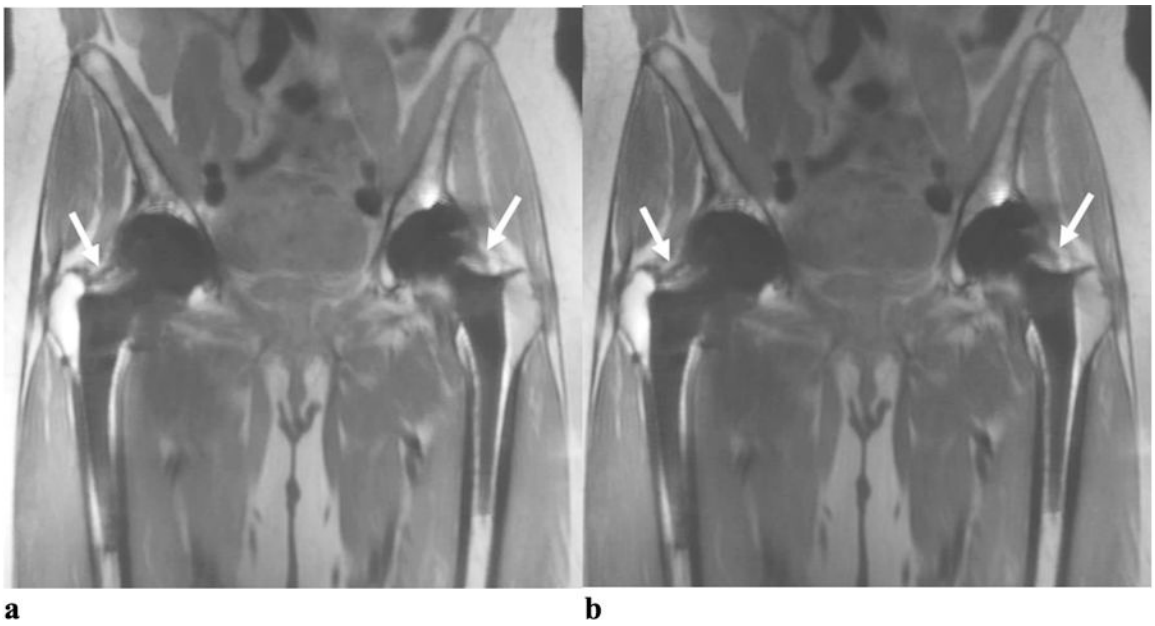


**Figure 5.**

(a) Coronal RPCA MAVRIC-SL and (b) Coronal MAVRIC-SL PD images in a 66-year old female with bilateral hip pain. For each hip both readers graded the overall image quality of both sequences as 4, the geometric distortion as 4 and the visualization of anatomy around the femoral and acetabular components as 4. Both readers thought that small joints effusions were probably present in both hips (arrows) for both sequences.

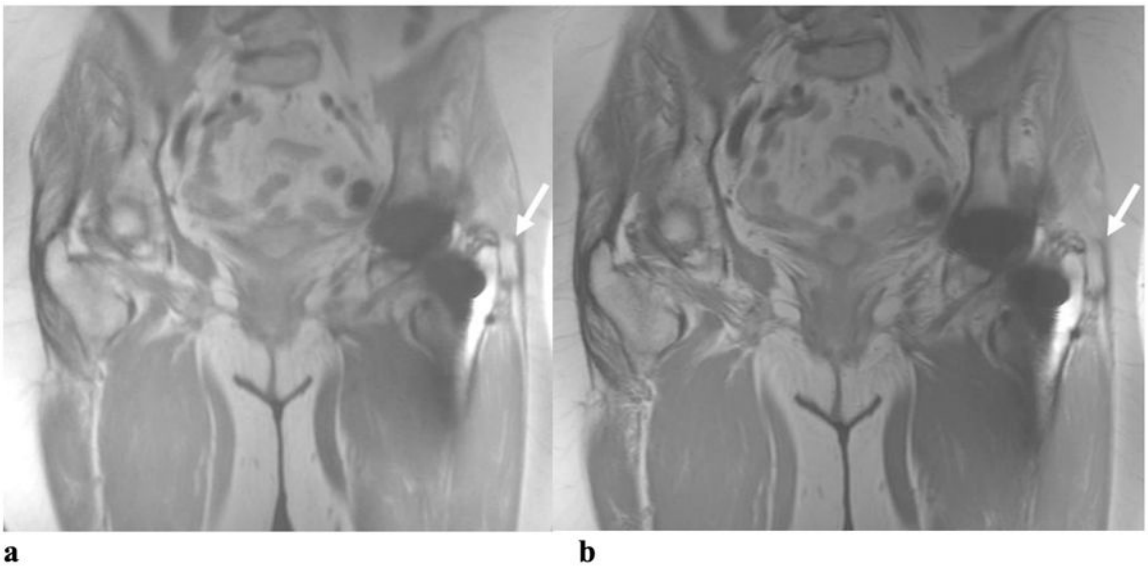


**Figure 6.**

(a) Coronal RPCA MAVRIC-SL and (b) Coronal MAVRIC-SL PD images in a 76-year old female with left hip pain. Both readers graded the overall image quality of RPCA MAVRIC-SL as 3 and conventional MAVRIC-SL as 4. In both sequences, geometric distortion was graded as 3 by both readers. Visualization of anatomic structures around the femoral and acetabular components was graded by Reader One as 3 on RPCA MAVRIC-SL and 4 on conventional MAVRIC-SL, but both were graded as 3 by Reader Two. Reader One thought that a small joint effusion was probably present on both RPCA MAVRIC-SL and conventional MAVRIC-SL, whilst Reader Two thought that a small joint effusion and trochanteric fluid collection was probably present on the RPCA sequence, but definitely present on conventional MAVRIC-SL (arrow). A joint effusion and trochanteric fluid collection were both seen on inversion recovery images in the original MRI study and the patient subsequently underwent a revision total hip arthroplasty for adverse local tissue reaction due to tribocorrosion.

**Table 1.**

Scoring system for qualitative parameters

| | |
|---|---|
| **Image Quality** | **5** - High contrast, with clear visibility of anatomic details and sharp contours<br>**4** - Mild loss of contrast without impairing visibility of anatomic details<br>**3** - Moderate contrast and mild blurring, mildly affecting discrimination of anatomic details<br>**2** - Moderate contrast and blurring with poor discrimination of anatomic details<br>**1** - Low contrast and blurry contours obscuring anatomic details |
| **Geometric Distortion** | **5** - Not present<br>**4** - Minimal distortion<br>**3** - Distortion mildly altering anatomic contours<br>**2** - Distortion severely impairing visualization of anatomic details near the metal implant<br>**1** - Severe distortion obscuring anatomic details adjacent to implant |
| **Visibility of Femur and Acetabulum** | **5** - Excellent visibility<br>**4** - Fully visible with slight blurring of borders<br>**3** - Visible but significant blurring of borders<br>**2** - Partially visible<br>**1** - Not visible |
| **Abnormal Imaging Findings** | **4** - Pathology definitely present<br>**3** - Pathology probably present<br>**2** - Pathology probably not present<br>**1** - Pathology definitely not present |

**Table 2.**

Comparison of mean scores between the Robust Principal Component Analysis (RPCA) technique and conventional MAVRIC-SL. Mean scores listed with standard deviation (SD) and p values, with $p<0.05$ considered statistically significant.

| | Image Quality | Geometric Distortion | Acetabular Visualization | Femoral Visualization | Extent of Artifact (Area in $cm^2$) |
|---|---|---|---|---|---|
| **RPCA-MAVRIC-SL** | 3.25 (SD 0.52) | 3.13 (SD 0.58) | 3.13 (SD 0.71) | 3.40 (SD 0.66) | 54.18 (SD 12.14) |
| **Conventional MAVRIC-SL** | 4.21 (SD 0.56) | 3.29 (SD 0.62) | 3.31 (SD 0.68) | 3.54 (SD 0.69) | 52.84 (SD 12.60) |
| **P-value** | <0.001 | 0.003 | 0.003 | 0.04 | 0.07 |

**Table 3.**

Inter-observer agreement for qualitative parameters. Gwet's agreement coefficients are shown. Values in parentheses represent the 95% confidence intervals. Interpretation of the agreement values per Landis and Koch criteria: almost perfect (0.8–1), substantial (0.6–0.8), moderate (0.4–0.6), fair (0.2–0.4), slight (0–0.2) and poor (<0) agreement.

| | Image Quality | Geometric Distortion | Acetabular Visualization | Femoral Visualization |
|---|---|---|---|---|
| **Conventional MAVRIC-SL** | 0.95 (0.85 – 0.99) | 0.98 (0.94 – 0.99) | 0.87 (0.77 – 0.97) | 0.92 (0.87 – 0.97) |
| **RPCA MAVRIC-SL** | 0.95 (0.84 – 0.99) | 0.91 (0.83 – 0.99) | 0.89 (0.79 – 0.99) | 0.78 (0.65 – 0.90) |